

Supporting Information

Pencil-like Hollow Carbon Nanotubes Embedded CoP-V₄P₃ Heterostructures as a Bifunctional Catalyst for Electrocatalytic Overall Water Splitting

Haiyang Chang ^{1,2,†}, Zhijian Liang ^{1,†}, Kun Lang ¹, Jiahui Fan ¹, Lei Ji ², Kejian Yang ², Shaolin Lu ², Zetong Ma ², Lei Wang ^{1,*} and Cheng Wang ^{1,2,*}

¹ Key Laboratory of Functional Inorganic Material Chemistry, Ministry of Education of the People's Republic of China, Heilongjiang University, Harbin 150080, China; 1202864@s.hlju.edu.cn (H.C.); 1202775@s.hlju.edu.cn (Z.L.); 1202866@s.hlju.edu.cn (K.L.); 2201434@s.hlju.edu.cn (J.F.)

² Jieyang Branch of Chemistry and Chemical Engineering Guangdong Laboratory, Jieyang 515200, China; jilei@gdut.edu.cn (L.J.); yangkj6@mail2.sysu.edu.cn (K.Y.); lushlin@gdut.edu.cn (S.L.); mazt@gdut.edu.cn (Z.M.)

* Correspondence: wanglei0525@hlju.edu.cn (L.W.); wangcheng@hlju.edu.cn (C.W.)

† These authors contributed equally to this work.

SEM images of CoVO

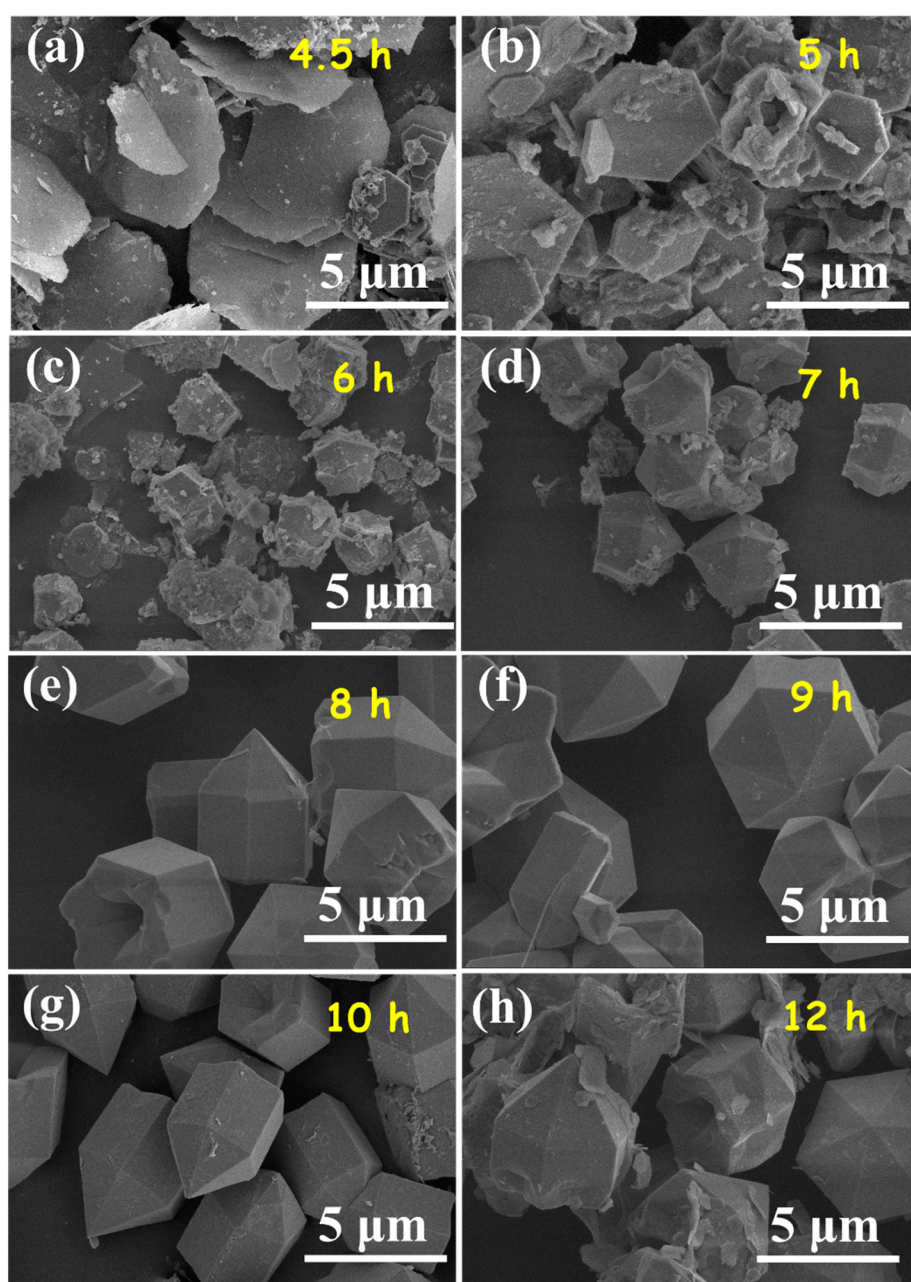


Figure S1. SEM images of CoVO synthesized by different hydrothermal reaction times.

SEM images of CoVO₁₀-CNT

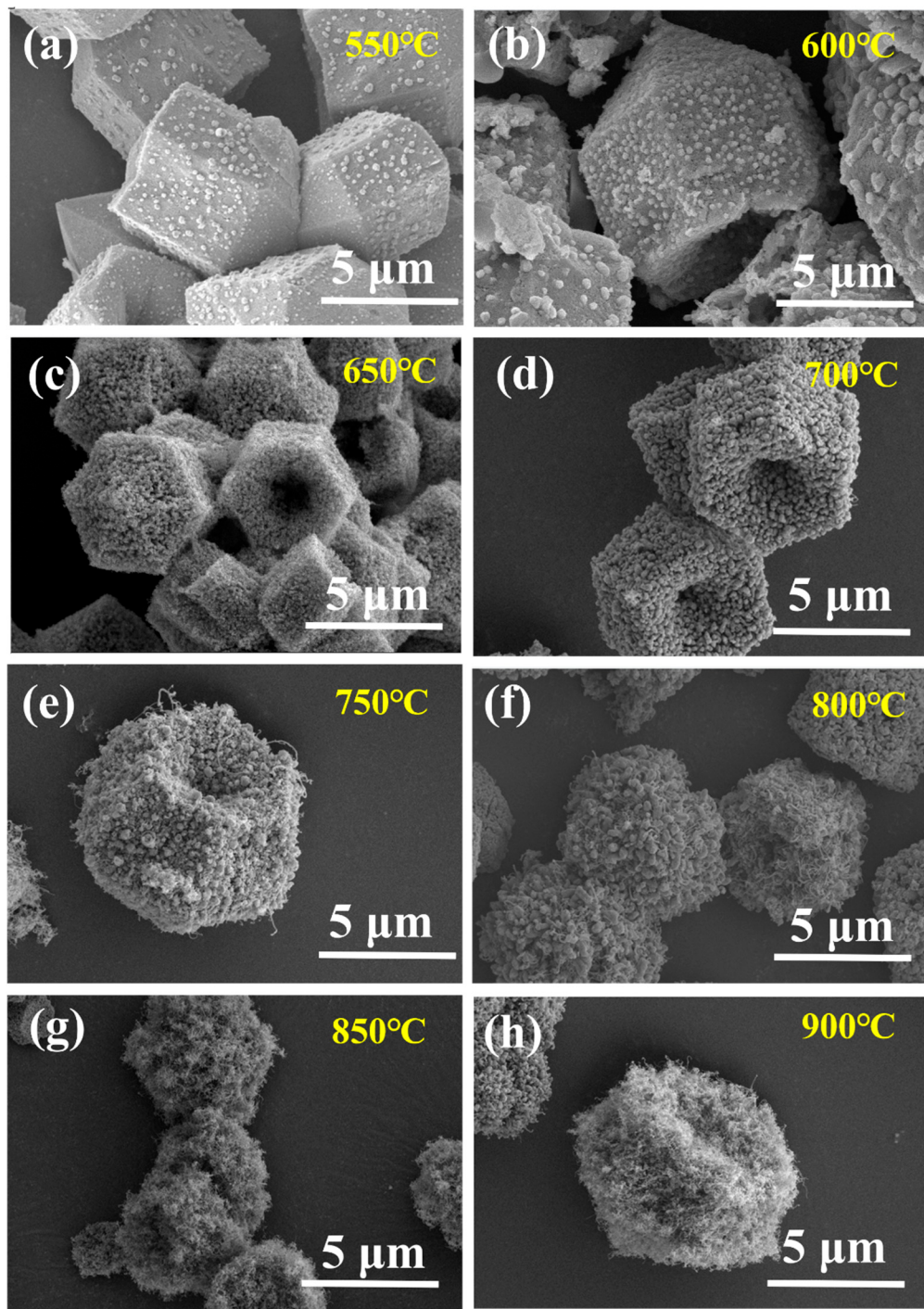


Figure S2. SEM images of CoVO₁₀-CNT synthesized by different vapor deposition calcination temperatures.

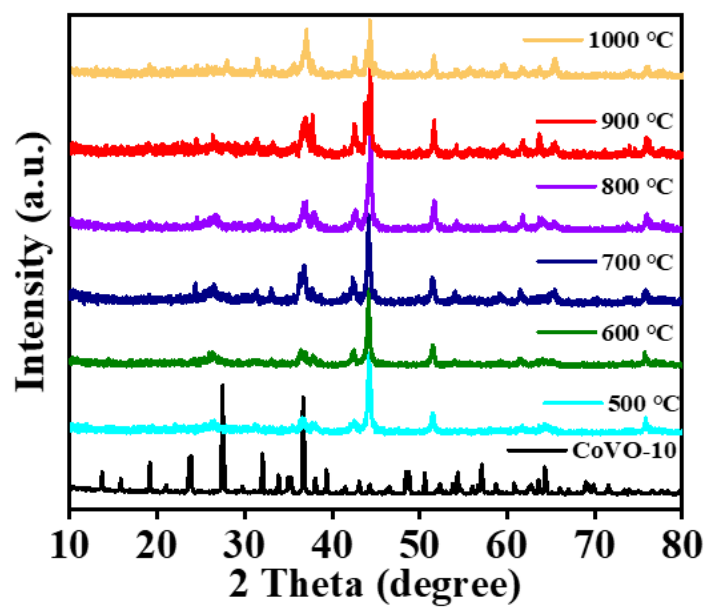


Figure S3. XRD patterns of the composites derived from CoVO-10 carbonized at different temperatures.

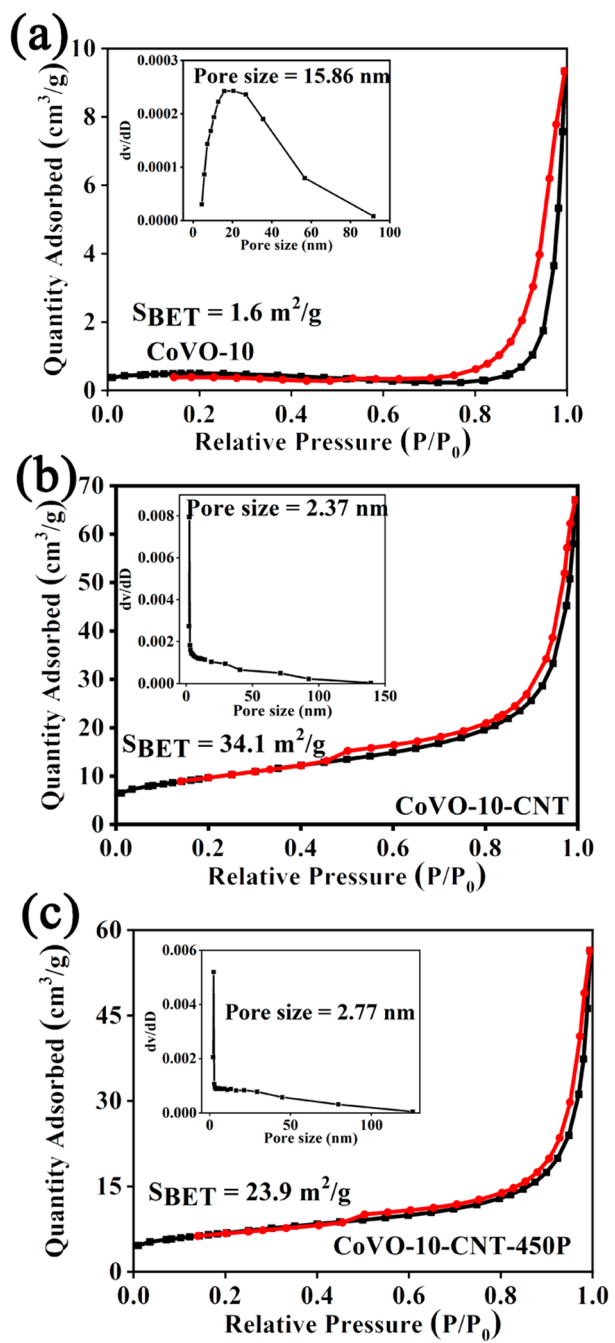


Figure S4. N_2 adsorption-desorption isotherms and corresponding BET surface areas of (a) CoVO-10, (b) CoVO-10-CNT and (c) CoVO-10-CNT-450P. The illustration shows the pore size distribution of the corresponding sample.

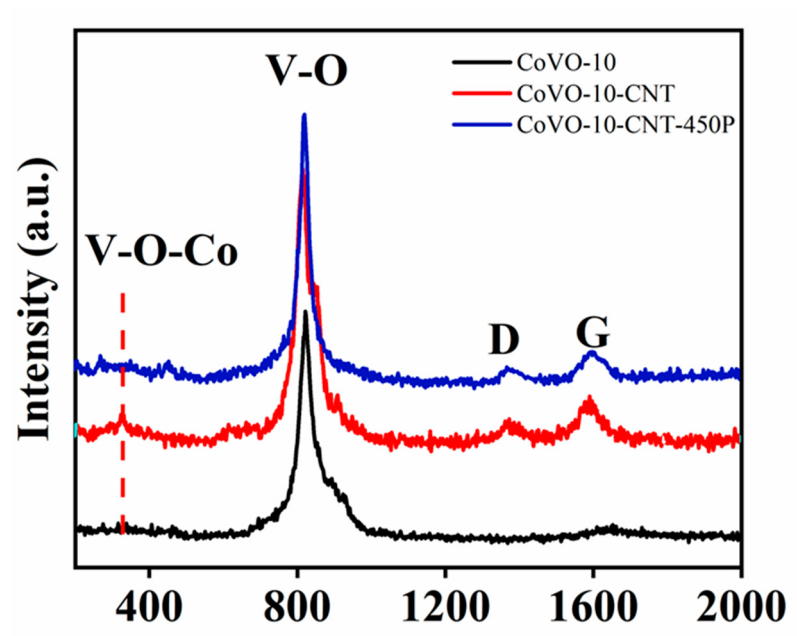


Figure S5. Raman spectra of different samples.

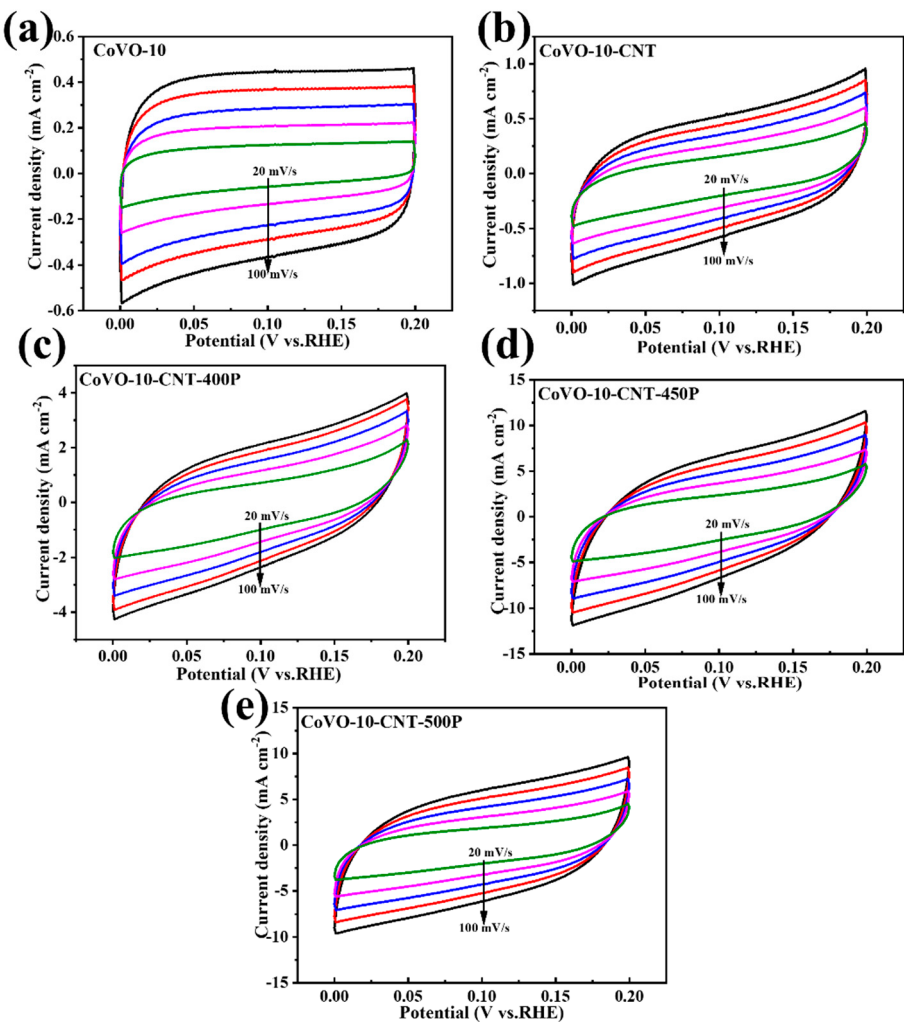


Figure S6. CV curves of different samples tested at $20\text{--}100 \text{ mV}\cdot\text{s}^{-1}$ in the potential range of $0\text{--}0.2\text{V}$.

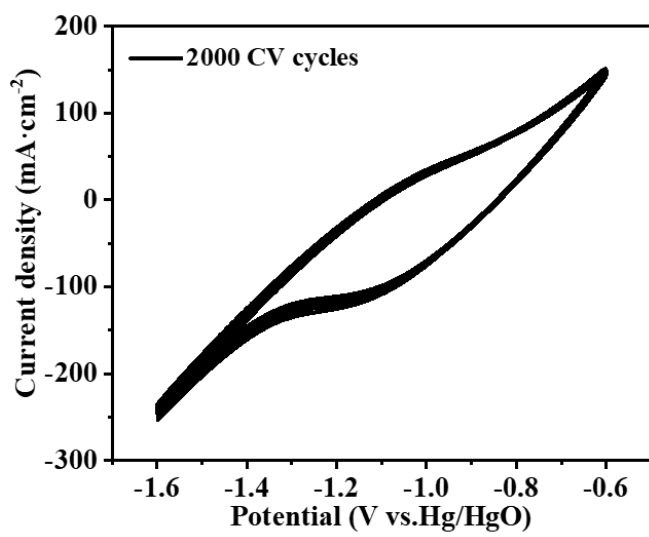


Figure S7. CV cycles of CoP/V₃P₄-CNT tested at the potential range of -1.6~−0.6 V.

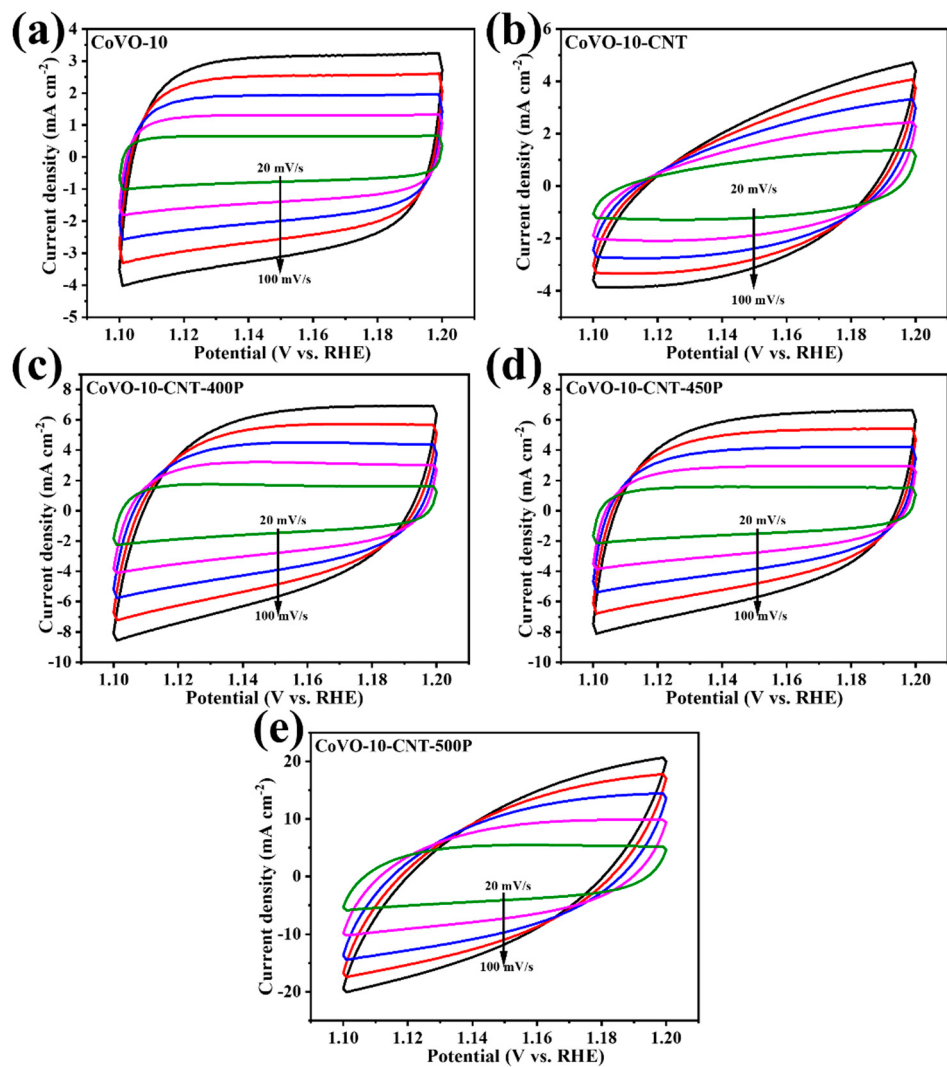


Figure S8. CV curve of different catalysts tested at 20–100 mV^{−1} in the potential range of 1.1–1.2 V.

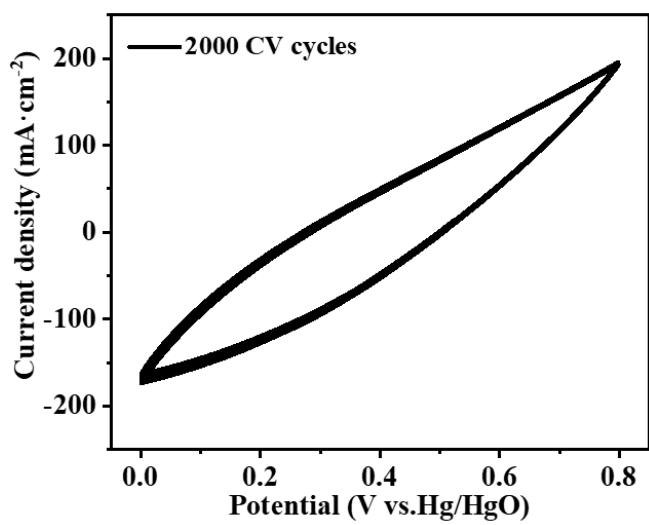


Figure S9. CV cycles of CoP/V₃P₄-CNT test in the potential range of 0–0.8 V.

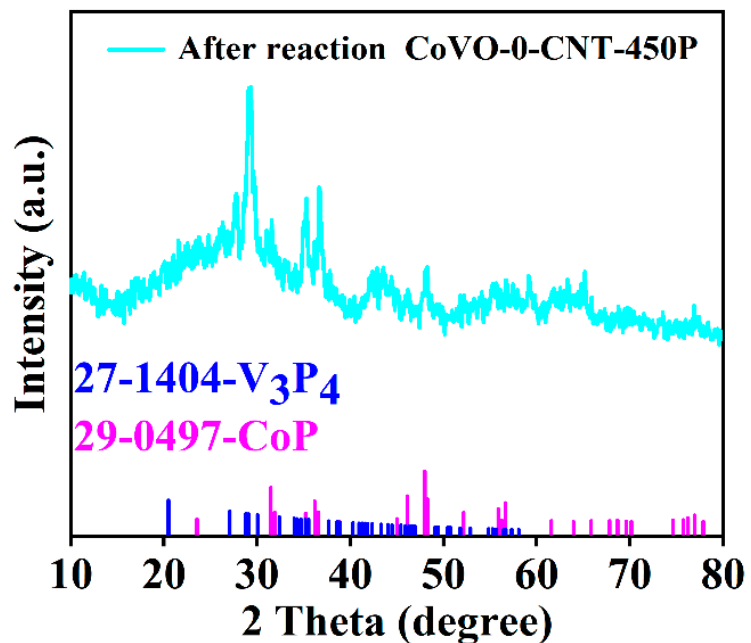


Figure S10. XRD pattern of CoVO-10-CNT-450P after stability test.

SEM images of CoVO-10-CNT-450P

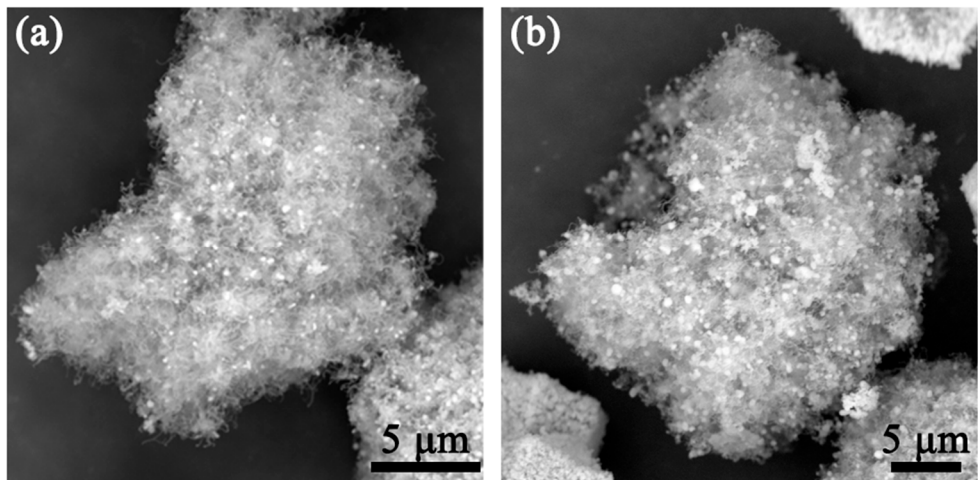


Figure S11. (a,b) SEM images of CoVO-10-CNT-450P after stability test.

XPS analyses of CoVO-10-CNT and CoVO-10-CNT-450P

Table S1. The element contents of Co, V, O, C and P elements in CoVO-10-CNT CoVO-10-CNT-450P determined by XPS analyses.

Sample	Content	Co	V	O	C	P
CoVO-10-CNT	At%	8.98	6.84	29.35	54.83	0
CoVO-10-CNT-450P	At%	8.38	6.84	27.20	52.49	5.09

Table S2. The resistance values for HER calculated from the EIS results of Figure 5e.

Catalyst	CoVO-10	CoVO-10- CNT	CoVO-10- CNT-400P	CoVO-10- CNT-450P	CoVO-10- CNT-500P
$R_s (\Omega)$	1.38	1.62	1.41	1.32	1.58
$R_{ct}(\Omega)$	8.05	5.27	4.11	2.63	3.12

Table S3. The resistance values for OER calculated from the EIS results of Figure 6e.

Catalyst	CoVO-10	CoVO-10- CNT	CoVO-10- CNT-400P	CoVO-10- CNT-450P	CoVO-10- CNT-500P
$R_s (\Omega)$	2.06	1.62	1.41	1.32	1.58
$R_{ct}(\Omega)$	16.35	11.68	9.69	5.85	7.16

Table S4. Performance comparison of recent non-noble metal bifunctional HER and OER electrocatalysts tested in 1.0 M KOH electrolyte.

Catalyst	$\eta_{\text{HER}}/\text{mV vs. RHE}$	$\eta_{\text{OER}}/\text{mV vs. RHE}$	References
	$10 \text{ mA}\cdot\text{cm}^{-2}$	$\text{mA}\cdot\text{cm}^{-2}$	
CoNi/MnO@CNTs	166	275	[13]
Co ₃ O ₄ @NiFe-LDH	79	215	[6]
Co _{5.47} N NP@N-PC	149	284	[2]
CoFe LDH-F/NF	166	260	[4]
Zn–Co–S nanoneedle/CFP	234	320	[11]
p-CoSe ₂ /CC	138	243	[9]
CoMo-LDH	115	290	[1]
CoP NS/CC	90	310	[14]
CoP ₃ NAs/CFP	119	334	[10]
Cu _{0.3} Co _{2.7} P/NC	220	190	[8]
CoP@SNC	174	350	[7]
CoP film	94	345	[3]
NixCo _{3-x} S ₄ /Ni ₃ S ₂ /NF	136	160	[12]
CoS ₂ HNSs	193	290	[5]
CoP/V₃P₄-CNT	124	280	This work

Table S5. Comparison the overall water splitting performance of CoVO-10-CNT-450P with previous reported superior bifunctional electrocatalysts tested in 1.0 M KOH.

Catalytic material	Voltage@10 mA cm ⁻²	Ref.
NiFeS@MXene/NF	1.57	[15]
Ni-Co-S film/Cu foam	1.67	[16]
NiFeRu-LDH	1.52	[17]
NiFe/NiCo ₂ O ₄ /Ni foam	1.67	[18]
Cu ₃ P NS/Ni foam	1.67	[19]
Mo ₂ C@C nanosheets	1.73	[20]
FeCo/Carbon paper	1.68	[21]
CoVO-10-CNT-450P	1.66	This work

References:

1. Bao, J.; Wang, Z.; Xie, J.; Xu, L.; Lei, F.; Guan, M.; Huang, Y.; Zhao, Y.; Xia, J.; Li, H. The CoMo-LDH Ultrathin Nanosheet as a Highly Active and Bifunctional Electrocatalyst for Overall Water Splitting. *Inorg. Chem. Front.* 2018, 5, 2964–2970.
2. Chen, Z.; Ha, Y.; Liu, Y.; Wang, H.; Yang, H.; Xu, H.; Li, Y.; Wu, R. In Situ Formation of Cobalt Nitrides/Graphitic Carbon Composites as Efficient Bifunctional Electrocatalysts for Overall Water Splitting. *ACS. Appl. Mater. Interf.* 2018, 10, 7134–7144.
3. Jiang, N.; You, B.; Sheng, M.; Sun, Y. Electrodeposited Cobalt-Phosphorous-Derived Films as Competent Bifunctional Catalysts for Overall Water Splitting. *Angew. Chem. Int. Ed.* 2015, 54, 6251–6254.
4. Liu, P.F.; Yang, S.; Zhang, B.; Yang, H.G. Defect-Rich Ultrathin Cobalt-Iron Layered Double Hydroxide for Electrochemical Overall Water Splitting. *ACS. Appl. Mater. Interf.* 2016, 8, 34474–34481.
5. Ma, X.; Zhang, W.; Deng, Y.; Zhong, C.; Hu, W.; Han, X. Phase and Composition Controlled Synthesis of Cobalt Sulfide Hollow Nanospheres for Electrocatalytic

- Water Splitting. *Nanoscale*. 2018, 10, 4816–4824.
- 6. Meng, L.; Xuan, H.; Wang, J.; Liang, X.; Li, Y.; Yang, J.; Han, P. Flower-Like $\text{Co}_3\text{O}_4@\text{NiFe-LDH}$ Nanosheets Enable High-Performance Bifunctionality Towards Both Electrocatalytic HER and OER in Alkaline Solution. *J. Alloy. Compd.* 2022, 919, 165877.
 - 7. Meng, T.; Hao, Y.-N.; Zheng, L.; Cao, M. Organophosphoric Acid-Derived CoP Quantum Dots@S,N-Codoped Graphite Carbon as a Trifunctional Electrocatalyst for Overall Water Splitting and Zn-Air Batteries. *Nanoscale* 2018, 10, 14613–14626.
 - 8. Song, J.; Zhu, C.; Xu, B.Z.; Fu, S.; Engelhard, M.H.; Ye, R.; Du, D.; Beckman, S.P.; Lin, Y. Bimetallic Cobalt-Based Phosphide Zeolitic Imidazolate Framework: CoPx Phase-Dependent Electrical Conductivity and Hydrogen Atom Adsorption Energy for Efficient Overall Water Splitting. *Adv. Energy. Mater.* 2017, 7, 1601555.
 - 9. Wan, S.; Jin, W.; Guo, X.; Mao, J.; Zheng, L.; Zhao, J.; Zhang, J.; Liu, H.; Tang, C. Self-Templating Construction of Porous CoSe_2 Nanosheet Arrays as Efficient Bifunctional Electrocatalysts for Overall Water Splitting. *ACS. Sustain. Chem. Eng.* 2018, 6, 15374–15382.
 - 10. Wu, T.; Pi, M.; Zhang, D.; Chen, S. 3D Structured Porous CoP_3 Nanoneedle Arrays as an Efficient Bifunctional Electrocatalyst for the Evolution Reaction of Hydrogen and Oxygen. *J. Mater. Chem. A* 2016, 4, 14539–14544.
 - 11. Wu, X.; Han, X.; Ma, X.; Zhang, W.; Deng, Y.; Zhong, C.; Hu, W. Morphology-Controllable Synthesis of Zn-Co-Mixed Sulfide Nanostructures on Carbon Fiber Paper Toward Efficient Rechargeable Zinc-Air Batteries and Water Electrolysis. *ACS. Appl. Mater. Inter.* 2017, 9, 12574–12583.
 - 12. Wu, Y.; Liu, Y.; Li, G.-D.; Zou, X.; Lian, X.; Wang, D.; Sun, L.; Asefa, T.; Zou, X. Efficient Electrocatalysis of Overall Water Splitting by Ultrasmall $\text{Ni}_x\text{Co}_{3-x}\text{S}_4$ Coupled Ni_3S_2 Nanosheet Arrays, *Nano. Energy*. 2017, 35, 161–170.
 - 13. Zhou, C.; Han, X.; Zhu, F.; Zhang, X.; Lu, Y.; Lang, J.; Cao, X.; Gu, H. Facile Synthesis of the Encapsulation of Co-Based Multimetallic Alloys/Oxide Nanoparticles Nitrogen-Doped Carbon Nanotubes as Electrocatalysts for the

- HER/OER. *Int. J. Hydrogen. Energ.* 2022, 47, 27775–27786.
- 14. Zhu, W.; Zhang, W.; Li, Y.; Yue, Z.; Ren, M.; Zhang, Y.; Saleh, N.M.; Wang, J. Energy-Efficient 1.67 V Single and 0.90 V Dual-Electrolyte Based Overall Water-Electrolysis Devices Enabled by a ZIF-L Derived Acid-Base Bifunctional Cobalt Phosphide Nanoarray. *J. Mater. Chem. A.* 2018, 6, 24277–24284.
 - 15. Chanda, D.; Kannan, K.; Gautam, J.; Meshesha, M. M.; Jang, S. G.; Dinh, V. A.; Yang, B. L., Effect of the Interfacial Electronic Coupling of Nickel-Iron Sulfide Nanosheets with Layer Ti₃C₂ MXenes as Efficient Bifunctional Electrocatalysts for Anion-Exchange Membrane Water Electrolysis. *Applied Catalysis B: Environmental* 2023, 321, 122039.
 - 16. Liu, T.; Sun, X.; Asiri, A. M.; He, Y., One-Step Electrodeposition of Ni–Co–S Nanosheets Film as a Bifunctional Electrocatalyst for Efficient Water Splitting. *Int. J. Hydrogen Energy* 2016, 41, 7264–7269.
 - 17. Chen, G.; Wang, T.; Zhang, J.; Liu, P.; Sun, H.; Zhuang, X.; Chen, M.; Feng, X., Accelerated Hydrogen Evolution Kinetics on NiFe-Layered Double Hydroxide Electrocatalysts by Tailoring Water Dissociation Active Sites. *Adv. Mater.* 2018, 30, 1706279.
 - 18. Xiao, C.; Li, Y.; Lu, X.; Zhao, C., Bifunctional Porous NiFe/NiCo₂O₄/Ni Foam Electrodes with Triple Hierarchy and Double Synergies for Efficient Whole Cell Water Splitting. *Adv. Funct. Mater.* 2016, 26, 3515–3523.
 - 19. Han, A.; Zhang, H.; Yuan, R.; Ji, H.; Du, P., Crystalline Copper Phosphide Nanosheets as an Efficient Janus Catalyst for Overall Water Splitting. *ACS Appl. Mater. Interfaces* 2017, 9, 2240–2248.
 - 20. Wang, H.; Cao, Y.; Sun, C.; Zou, G.; Huang, J.; Kuai, X.; Zhao, J.; Gao, L., Strongly Coupled Molybdenum Carbide on Carbon Sheets as a Bifunctional Electrocatalyst for Overall Water Splitting. *ChemSusChem* 2017, 10, 3523–3523.
 - 21. Liu, W.; Du, K.; Liu, L.; Zhang, J.; Zhu, Z.; Shao, Y.; Li, M., One-Step Electroreductively Deposited Iron-Cobalt Composite Films as Efficient Bifunctional Electrocatalysts for Overall Water Splitting. *Nano Energy* 2017, 38, 576–584.